

## Biological Activity and Bio-Sorption Properties of the Ti<sub>2</sub>C Studied by Means of Zeta Potential and SEM

A. Jastrzębska<sup>1,\*</sup>, E. Karwowska<sup>2</sup>, D. Basiak<sup>3</sup>, A. Zawada<sup>1</sup>, W. Ziemkowska<sup>3</sup>, T. Wojciechowski<sup>3</sup>, D. Jakubowska<sup>1</sup>, A. Olszyna<sup>1</sup>

<sup>1</sup> Warsaw University of Technology, Faculty of Materials Science and Engineering, 02-507 Warsaw, Woloska 141, Poland,

<sup>2</sup> Warsaw University of Technology, Faculty of Environmental Engineering, 00-653 Warsaw, Nowowiejska 20, Poland

<sup>3</sup> Warsaw University of Technology, Faculty of Chemistry, 00-664 Warsaw, Noakowskiego 3, Poland

\*E-mail: [agsolgala@gmail.com](mailto:agsolgala@gmail.com)

Received: 7 September 2016 / Accepted: 27 December 2016 / Published: 12 February 2017

---

The expanded Ti<sub>2</sub>C MXene phase was synthesized from the commercial Ti<sub>2</sub>AlC MAX phase using classical acidic aluminium extraction method. The individual expanded Ti<sub>2</sub>C sheets were characterized by the diameters of between 26 and 61 nm and formed the specific network of slit-shaped pores in the size range of 3–5 nm. The BET specific surface area of expanded Ti<sub>2</sub>C was ca. 42% higher in comparison with layered Ti<sub>2</sub>AlC. Our investigations results revealed that both Ti<sub>2</sub>AlC and Ti<sub>2</sub>C phases did not influence negatively the gram-positive bacteria commonly occurring in the natural environment. Moreover, the slightly intensified growth of *Bacillus sp.* strain was observed in the vicinity of tested Ti<sub>2</sub>AlC and Ti<sub>2</sub>C. The SEM investigations of the preferential sites for bacteria adsorption indicated the presence of minor apoptosis for only *Bacillus sp.* strain, especially when the cells were located between individual sheets of the expanded Ti<sub>2</sub>C. The zeta potential curves obtained for Ti<sub>2</sub>AlC and Ti<sub>2</sub>C in distilled water differed significantly in shape. The intensive peak towards zero zeta potential was observed for Ti<sub>2</sub>C. Adsorption of bacteria cells on Ti<sub>2</sub>C resulted in changing of its zeta potential to that of bacteria cells.

---

**Keywords:** Ti<sub>2</sub>C, MXene, zeta potential, bio-activity, biocidal

### 1. INTRODUCTION

Recently, the layered early transition metal carbides and nitrides (called MAX phases) have been first introduced by Barsoum et al. [1]. Since that time, MAX phases have attracted the interest of academia and industry due to the fact that they allow to achieve a dramatic improvement in mechanical

properties of materials [2, 3]. Chemically expanded structures of early transition metal carbides, known as MXenes, are novel and poorly studied family of materials characterized by specific properties which can be described as characteristic for both metals and ceramics [4]. These unique properties made the applicability of MXenes very attractive in the high-tech area of science. It should be however noted, that the potential for the biological activity of MXenes have not yet been fully discovered, highly limiting the possibility of their application in many fields of bioscience and biotechnology. So far, only Wang *et al.* [5] discovered that MXenes exhibited effective immobilization of enzymes and biocompatibility for red-ox proteins. This indicates the promise for applications in electrochemical biosensors. However still, there are no reports on antimicrobial and bio-sorption properties of MXenes. The present study, for the first time, investigates the biological activity of  $Ti_2C$ , which is the expanded form of layered titanium carbide ( $Ti_2AlC$ ) against gram-positive bacteria such as *Bacillus sp.*, *S. aureus* and *Sarcina*. The aim of this study was also to describe the preferential sites for adsorption of the bacteria cells using scanning electron microscope examinations as well as analysis of changes of zeta potential of expanded  $Ti_2C$  MXene as a result of bacteria cells adsorption.

## 2. EXPERIMENTAL

### 2.1. Synthesis procedure of the expanded $Ti_2C$ (MXene)

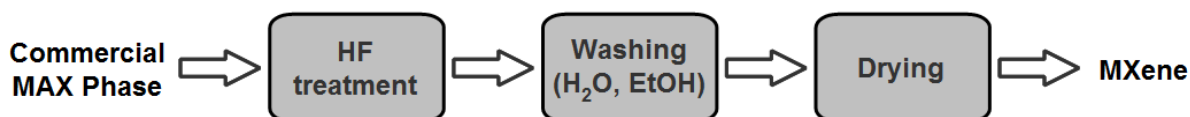


**Figure 1.** Flowchart of the technological stages of the synthesis process of  $Ti_2C$  MXene phase from  $Ti_2AlC$  commercial MAX phase.

The layered  $Ti_2AlC$  was purchased from Kanthal (the Sandvik AB group), Sweden. The composition of  $Ti_2AlC$  as declared by a manufacturer was as following: 5-10 wt% of carbon, 20-25 wt% of aluminium and balanced wt% of titanium.

The technological stages of the synthesis process of  $Ti_2C$  MXene phase from  $Ti_2AlC$  commercial MAX phase were presented in Fig. 1. The  $Ti_2AlC$  commercial MAX phase powder was immersed in 48% hydrofluoric acid (Sigma-Aldrich) for 24 h at room temperature. About 10 ml of hydrofluoric acid was used for 1 g of starting material. The resulting sediment was washed four times using deionized water and four times with technical grade ethanol. The solid product of the layered  $Ti_2C$  was dried overnight in room temperature.

### 2.2. Characterization of the morphology and structure

The morphologies of the surface of layered  $Ti_2AlC$  (MAX phase) and its expanded form -  $Ti_2C$  (MXene phase) were analyzed using scanning electron microscope (SEM) of LEO 1530, Zeiss, USA.

The microscope operated at 2.0kV. The tested powders were directly deposited on the surface of a carbon tape and subsequently coated with a thin carbon layer (BAL-TEC SCD 005 duster with a CEA 035 unit). Then, the obtained samples were subjected to the analysis of morphology. The elemental composition in layered  $Ti_2AlC$  and expanded  $Ti_2C$  was analyzed using energy dispersive X-ray spectroscopy (EDS, coupled with SEM) allowing to obtain the information on the elements content in a given region. The X-ray diffraction (XRD) was used for phase analysis at room temperature (Bruker D8 Advance) with Cu  $K\alpha$  radiation ( $\lambda=0.154056$  nm) and voltage of 40 kV (40 mA). The angle  $2\theta$  range was chosen from  $15^\circ$  to  $120^\circ$ . The step  $\Delta 2\theta$  was 0.025 together with counting time of 3 s. Subsequently, the obtained XRD patterns were analysed using the software of Bruker EVA.

### 2.3. Analysis of physical properties and porous structure

The analysis of physical properties and porous structure of layered  $Ti_2AlC$  and expanded  $Ti_2C$  were examined using the physical nitrogen sorption isotherms  $V=f(p/p^o)$  which relates to the volume of the adsorbed gaseous  $N_2$  as a function of  $N_2$  relative pressure. The isotherms were measured experimentally using a Quadrasorb-SI device from Quantachrome Instruments, USA. Before the measurements, the samples were degassed in vacuum at a temperature of  $300^\circ C$  for 24 hours. The isotherms of adsorption and desorption of gaseous  $N_2$  on the surface of tested samples were recorded for the entire relative pressure range ( $p/p^o$  from 0 to 1) at a temperature of liquid nitrogen bath i.e.  $-195.8^\circ C$ . The specific surface area,  $S_{BET}$  was obtained using the method of Brunauer, Emmett, and Teller (BET) within the relative pressure range of 0,05-0,35. The shape of the obtained isotherms was also analysed. It represents the shapes of pores that are present in the tested material. The total volume of the pores,  $V_{pores}$  and the surface area occupied by the pores  $S_{pores}$  was determined using the method of Barret, Joyner, and Halenda (BJH). The assumption related to the BJH method is that, at the relative pressure  $< 0,4$ , during the capillary condensation in pores the only effect that is observed together with a further increase of the pressure is the thickening of the  $N_2$  mono-layer. This mono-layer is formed on the pore walls surface. The average pore size,  $D_{BJH}$  was estimated from the distributions of the pore sizes.

### 2.4. Analysis of potential antimicrobial properties

The bioactivities of layered  $Ti_2AlC$  and expanded  $Ti_2C$  were tested qualitatively (agar diffusion method) using the selected gram-positive bacteria strains of *Bacillus sp.*, *Staphylococcus aureus* and *Sarcina* which were taken from the private collection of microorganisms of the Biology Department, Faculty of Environmental Engineering, Warsaw University of Technology. On the surface of Petri dishes with solid nutrient agar (Merck) there were inoculated lines of microorganisms. The tested powders were then located in the area of the spread lines and the samples were then incubated for 48h at different temperatures i.e.  $26^\circ C$  or  $37^\circ C$ , which were dependent on the bacterial species. After incubation, the Petri plates were photographed which allowed for observations of the growth inhibition zones.

### 2.5. Analysis of preferential sites for bacteria adsorption

The qualitative analysis of preferential sites for adsorption of bacteria cells on the surface of expanded  $Ti_2C$  was investigated using scanning electron microscope examination with the same bacteria strains used as in agar diffusion method i.e.: *Staphylococcus aureus*, *Bacillus sp.*, and *Sarcina*. Before analysis, microorganisms were spread on the nutrient agar (Merck) and cultivated for 24 h at  $37^\circ C$ . Drinking water was filtered before use with  $0,2 \mu m$  sterile syringe filter (Whatman). Then, the bacterial cells were harvested from Petri plates and transferred to the drinking water due to obtain cells density of about  $10^5-10^6$  cells/ml. Subsequently, the such prepared bacteria stock suspension was incubated at  $37^\circ C$  for 5 minutes. Subsequently,  $200 \mu L$  of each suspensions of bacteria were transferred to  $5 \times 10^{-5} g/200 \mu L$  suspensions of  $Ti_2C$  powder in drinking water. The such prepared mixtures of  $Ti_2C$  powder and bacteria cells were incubated in  $37^\circ C$  for 30 minutes. After that time,  $100 \mu L$  of 20 wt% water solution of glutaraldehyde was added to each suspension which was then left for spontaneous sedimentation. After 1 hour, the clarified solution from above each of the the sedimented powder was removed and changed for the  $500 \mu L$  of the first of series of graded concentrations of ethanol (20 wt%). Subsequently, 40, 60, 80 and 98 wt% ethanol was used for rinsing the powder samples. The samples were then dried and deposited on a carbon tape. Next, the samples were coated with a thin carbon layer and were subjected to SEM analysis (LEO 1530, Zeiss, USA). The SEM examinations were conducted under 3.0kV.

### 2.6. Zeta potential analysis

The zeta potential ( $\zeta$ ) of the layered  $Ti_2AlC$  and expanded  $Ti_2C$  powder in the distilled and drinking water environment was analyzed using Zetasizer Nano ZS (Malvern Instruments), equipped with an MPT-2 automatic titrator and a titration media degasser. Drinking water was purified as described in 2.5. Then, the zeta potential was determined using Smoluchowski's rule based on the electrophoretic mobility ( $\mu$ ).

The  $\zeta$  analysis was first performed both in distilled water as well as drinking water environment in the pH range from 4 to 10 which enabled the determination of IEP value (isoelectric point) for each powder in the specific environment. The test samples were  $0,5 mg/10 mL$  suspensions of  $Ti_2C$  and  $Ti_2AlC$ . The  $Ti_2AlC$  was used as a non-expanded reference material. Before the measurement, the samples were mixed for 5 seconds and then transferred to a polystyrene U-shaped cells (Malvern Instruments). In the next step, the cells were stabilized at  $25^\circ C$  for 5 seconds. Finally, every measurement was conducted at  $25^\circ C$ , and repeated 10 times. The sodium hydroxide (0.1 M NaOH) and hydrochloric acid (0.1 M HCl) were used as the titration media.

Due to allow the observation of the changes of electrical charge which is formed on the surface of the analyzed powders in presence of bacterial cells, the measurements of the zeta potential were conducted in drinking water environment, separately for: (i)  $0,5 mg/10 mL$  suspensions of  $Ti_2AlC$  and  $Ti_2C$  powders; (ii)  $100 \mu L/10 mL$  suspensions of pure bacteria cells; (iii) mixed suspensions of powders and bacteria cells. The samples of pure bacteria cells were stabilized before measurement at  $25^\circ C$  for 1 minute. The mixed suspensions of powders and bacteria were incubated at  $37^\circ C$  for 5

minutes with 100 rpm stirring rate. Then, the samples were stabilized at a temperature of 25 °C for 1 minute and the electrophoretic mobility was measured. It should be noted, that each of the zeta potential measurements was an average of 100 repetitions.

### 3. RESULTS AND DISCUSSION

The morphologies of layered  $\text{Ti}_2\text{AlC}$  and expanded  $\text{Ti}_2\text{C}$  were examined using a scanning electron microscope (SEM) and were presented in Fig. 2.

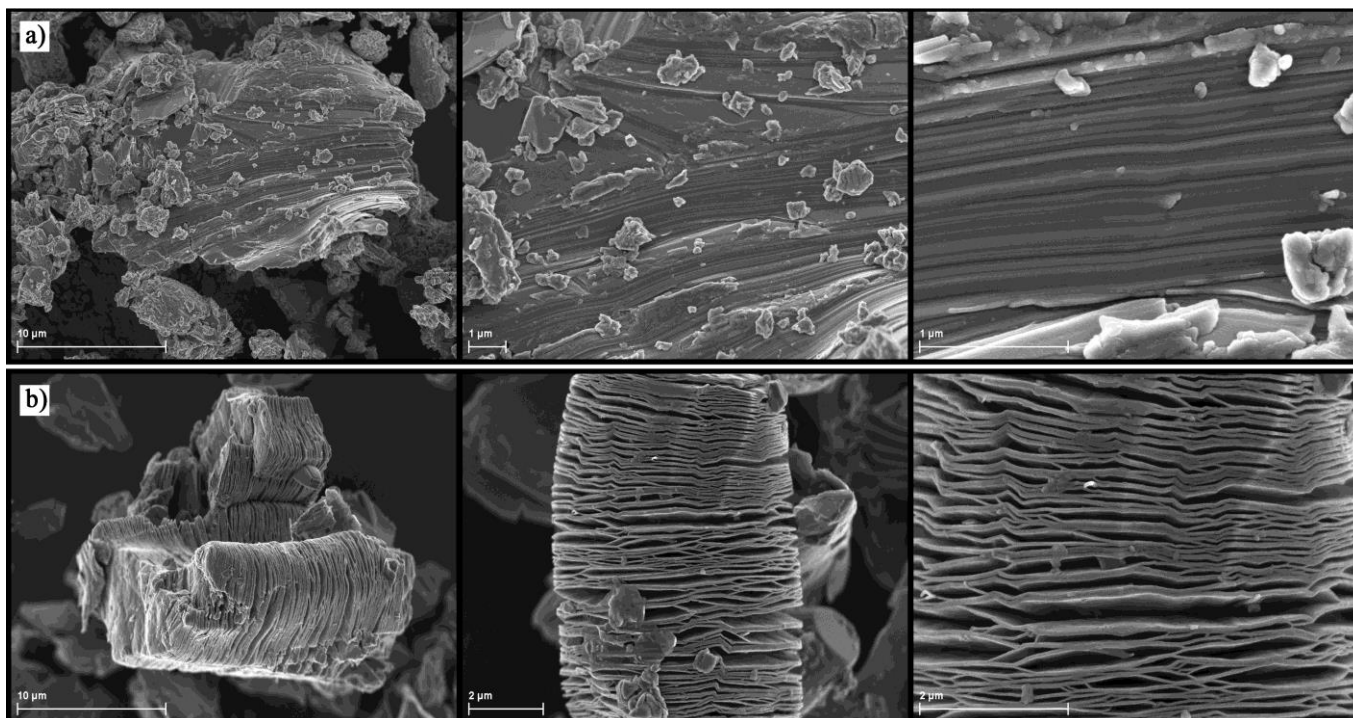


**Figure 2.** The set of SEM images obtained for the  $\text{Ti}_2\text{AlC}$  a) and expanded  $\text{Ti}_2\text{C}$  b).

One can notice that the  $\text{Ti}_2\text{AlC}$  grains possessed non-regular shapes (Fig. 2a). The high magnification images confirmed the layered structure of  $\text{Ti}_2\text{AlC}$  used as a substrate for  $\text{Ti}_2\text{C}$  synthesis. The SEM observations also showed that the sizes of the large  $\text{Ti}_2\text{AlC}$  grains were generally below 20 μm. It can be also noticed the large amount of fraction of small particles (below 2 μm) which were not characterized by the layered structure. It should be noted that they were almost completely removed during the rinsing procedure due to obtain the pure  $\text{Ti}_2\text{C}$  material which morphology was presented in Fig. 2b. As can be seen, the layers of the dense  $\text{Ti}_2\text{AlC}$  grains were successfully split into individual sheets of the expanded  $\text{Ti}_2\text{C}$ . The SEM results also indicate that the widths of the grains located perpendicular to the surface of the sheets were significantly extended in comparison to  $\text{Ti}_2\text{AlC}$  grains.

The high magnification SEM images presenting in detail the morphologies of the  $\text{Ti}_2\text{C}$  sheets were shown in Fig. 3. The qualitative analysis of sheets diameters indicated that the measured thickness varied between 26 and 61 nm. The sheets possessed the relatively sharp edges and were

connected to each other by specific bridges, forming the stable stack of nano-sized sheets with the slit-shaped pores.

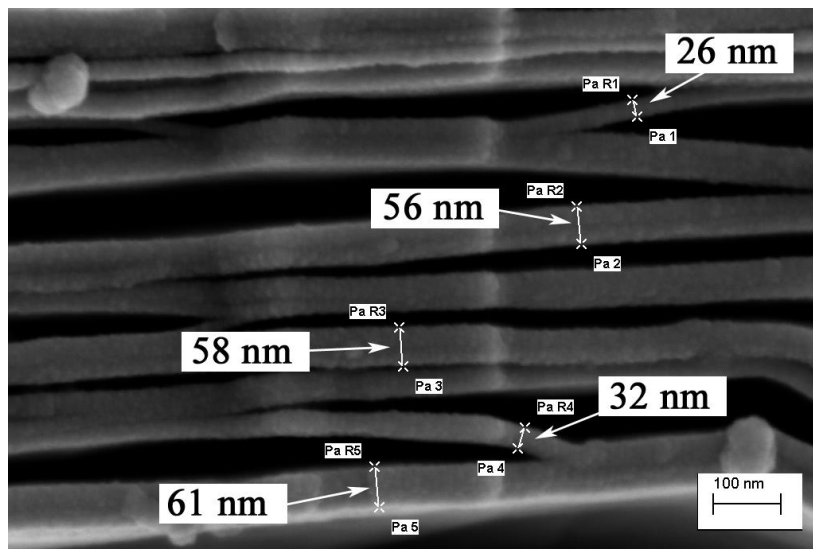


**Figure 3.** High magnification SEM image obtained for the expanded  $Ti_2C$ , added with the analysis of sheets diameters.

The elemental composition of the layered  $Ti_2AlC$  and expanded  $Ti_2C$  was also confirmed using the EDS analysis (Energy Dispersive X-ray Spectroscopy). The corresponding electron diffractions were presented in Fig. 4. The EDS results of the  $Ti_2AlC$  showed the presence of titanium, aluminium and carbon (Fig. 4a) whereas for  $Ti_2C$  almost no aluminium was detected (Fig. 4b).

**Table 1.** Summary of EDS results obtained from the surface of  $Ti_2AlC$  particle.

element	Series	C [at%]	C[wt%]	C error [wt%]
titanium	K-series	68,03	42,24	6,08
aluminium	K-series	15,55	17,14	2,28
carbon	K-series	16,41	40,63	7,39

The EDS results for each of the samples were also summarized in Tab. 1 and 2. As can be seen, the amount of aluminium was reduced from c.a. 17 wt% in  $Ti_2AlC$  (Tab. 1) to almost 0 wt% in  $Ti_2C$  (Tab. 2) which confirmed the efficiency of the chemical process of acidic aluminium extraction from  $Ti_2AlC$ . The EDS results obtained for  $Ti_2C$  have also shown the presence of significant amounts of elements such as: oxygen (19,6 wt %) and fluorine (12,2 wt %) which were previously described by other researchers [4, 6]. Other elements such as: calcium, sodium, sulfur, phosphorus and magnesium were present in  $Ti_2C$  in amounts around 1 wt% which were within the standard deviation of measurement (Tab. 2). Their presence may be considered as negligible impurities introduced during chemical process of aluminium extraction or rinsing.

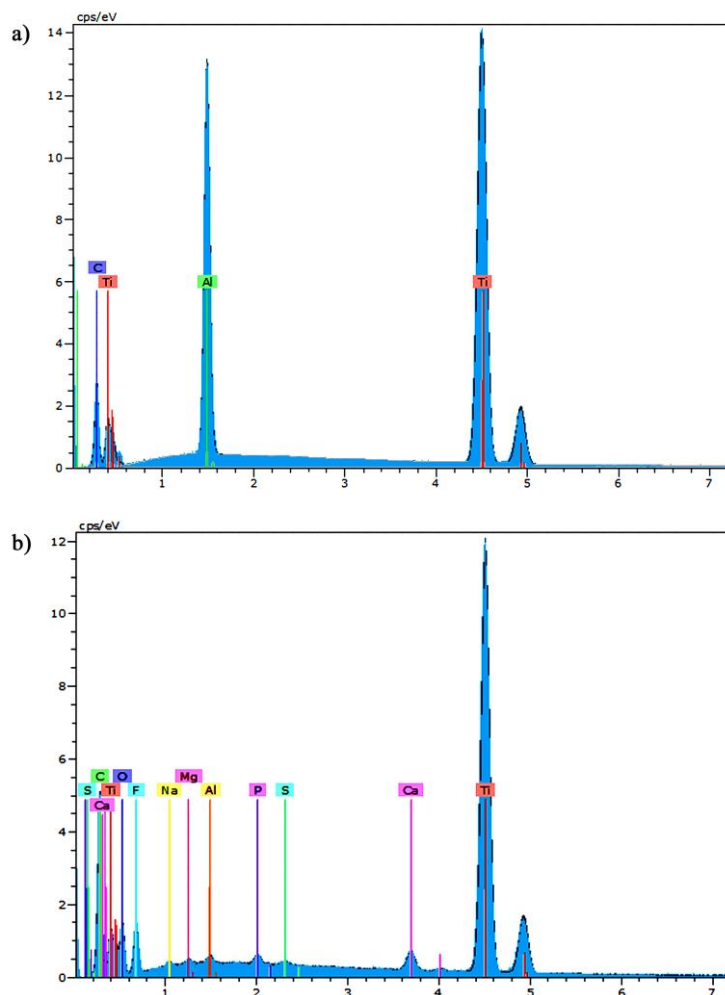


**Figure 4.** Results of EDS analysis obtained from the surface of  $Ti_2AlC$  grain a) and expanded  $Ti_2C$  sheets b).

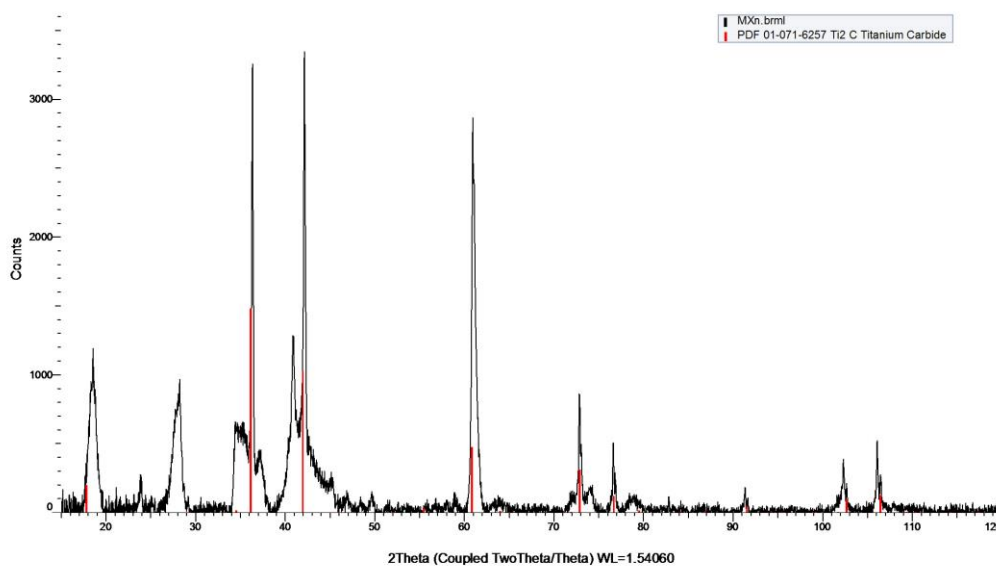


**Figure 5.** The XRD pattern obtained for  $Ti_2C$  sample.

It is also very highly possible, that those impurities were actually present from the beginning in the commercial MAX phase, but could not be detected by EDS due to the high amount of aluminium. After its removal, they become detectable by EDS detector. It should be noted, that we are the first who presented the EDS results showing that, in spite of using the pure HF for aluminium extraction, some minor impurities can be detected by EDS analysis in the final product. The XRD pattern obtained for the analysed sample was presented in Fig. 5. The obtained diffractogram confirmed the presence of the  $Ti_2C$  phase.

**Table 2.** Summary of EDS results obtained from the surface of  $Ti_2C$  sheets.

element	Series	C [at%]	C [wt%]	C error [wt%]
titanium	K-series	55,76	28,01	5,53
aluminium	K-series	0,24	0,21	0,13
carbon	K-series	19,23	38,50	8,55
oxygen	K-series	13,05	19,62	6,91
fluorine	K-series	9,64	12,20	5,03
calcium	K-series	1,33	0,80	0,23
sodium	K-series	0,17	0,17	0,13
sulfur	K-series	0,15	0,11	0,10
phosphorus	K-series	0,31	0,24	0,13
magnesium	K-series	0,14	0,14	0,11

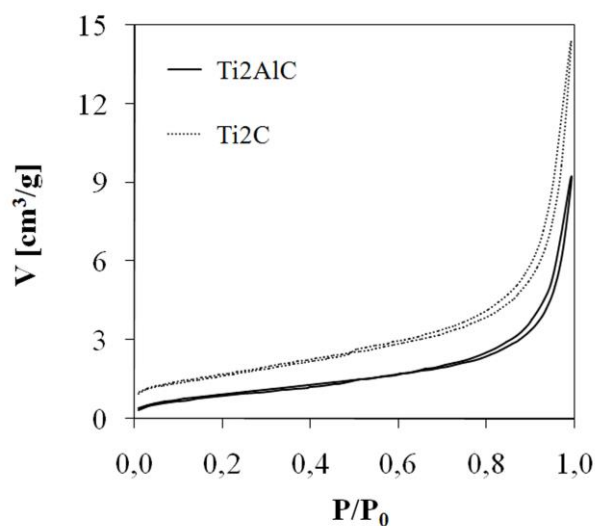


**Figure 6.** Nitrogen sorption isotherms obtained for the  $Ti_2AlC$  a) and expanded  $Ti_2C$  b).

The analysis of physical properties and porous structure of layered  $Ti_2AlC$  and expanded  $Ti_2C$  were examined based on the isotherms of the physical nitrogen sorption. The obtained isotherms are given in Fig. 6. The obtained results indicate, that the expanded  $Ti_2C$  adsorbed significantly more nitrogen in comparison go  $Ti_2AlC$ . The shape of the obtained isotherms suggested the presence of slit pores which are also characteristic for graphenes [7, 8].

The results of the physical properties of layered Ti<sub>2</sub>AlC and expanded Ti<sub>2</sub>C were summarized in Table 3. As expected, the BET specific surface area of expanded Ti<sub>2</sub>C was ca. 42% higher in comparison with layered Ti<sub>2</sub>AlC. In particular, the significant increase in the surface area is related to the formation of large number of slit-pores in Ti<sub>2</sub>C as a result of expanding process. The results of the total volume of pores ( $V_{BJH}$ ) also confirmed this assumption. The value of  $V_{BJH}$  obtained for Ti<sub>2</sub>C was ca. 0,007 cm<sup>3</sup>/g larger in comparison with Ti<sub>2</sub>AlC (Tab. 3).

**Table 3.** Physical properties of the Ti<sub>2</sub>AlC and expanded Ti<sub>2</sub>C.

sample name	$S_{BET}$ [m <sup>2</sup> /g]	$S_{pores}$ [m <sup>2</sup> /g]	$V_{pores}$ [cm <sup>3</sup> /g]	$D_{pore}$ [nm]
Ti <sub>2</sub> AlC	3,51	3,01	0,014	4
Ti <sub>2</sub> C	6,09	4,74	0,021	4

The pore size distributions obtained for Ti<sub>2</sub>AlC and Ti<sub>2</sub>C are presented in Fig. 7. The obtained BJH results indicate that, in all of our materials, there were mainly nanopores (in the range of 3–5 nm) present. As can be also observed, the mesopores (in the range of 5–50 nm) were present in great minority in comparison to the general amount of nanopores.

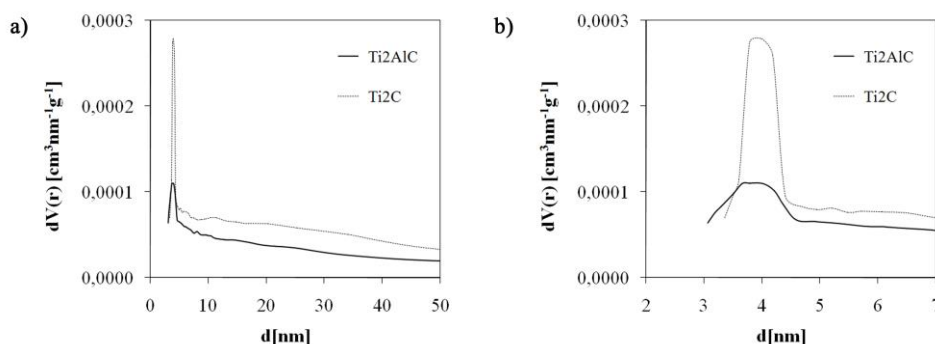


**Figure 7.** The distributions of pore diameter obtained using BJH method for the Ti<sub>2</sub>AlC a) and expanded Ti<sub>2</sub>C b).

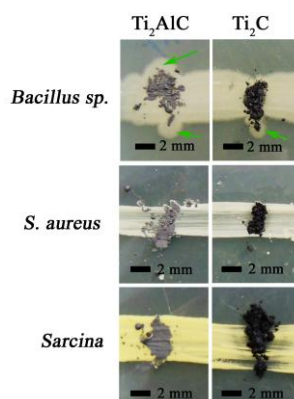


**Figure 8.** Photographs of the surface of Petri plates, presenting the growth of: *Bacillus sp.*, *S. aureus* and *Sarcina* bacteria in presence of Ti<sub>2</sub>AlC and expanded Ti<sub>2</sub>C. Green arrows mark regions where microorganisms exceed their primary inoculation line.

The present study also investigates the bioactive properties of  $Ti_2C$ , which is the expanded form of layered titanium carbide ( $Ti_2AlC$ ). The investigations of the bioactive properties of the samples were performed using the classical culture method. Due to enable comparison, the layered  $Ti_2AlC$  was also subjected for microbiological analysis. As can be seen in Fig. 8, no inhibition of bacterial growth was observed in the presence of the tested samples. However, in case of *Bacillus sp.* bacteria the intensified growth was observed in the area directly surrounding the applied sample. As a result, the *Bacillus sp.* bacteria exceeded their primary growth lines. This effect may be related to the presence of the specific adhesion mechanisms between microorganisms and a specific surface properties of the tested material. For further studies, the expanded form of  $Ti_2C$  was used. The results of the qualitative analysis of preferential sites for adsorption of bacteria cells on the surface of expanded  $Ti_2C$  partially confirmed the described observations of the specific adhesion mechanisms.

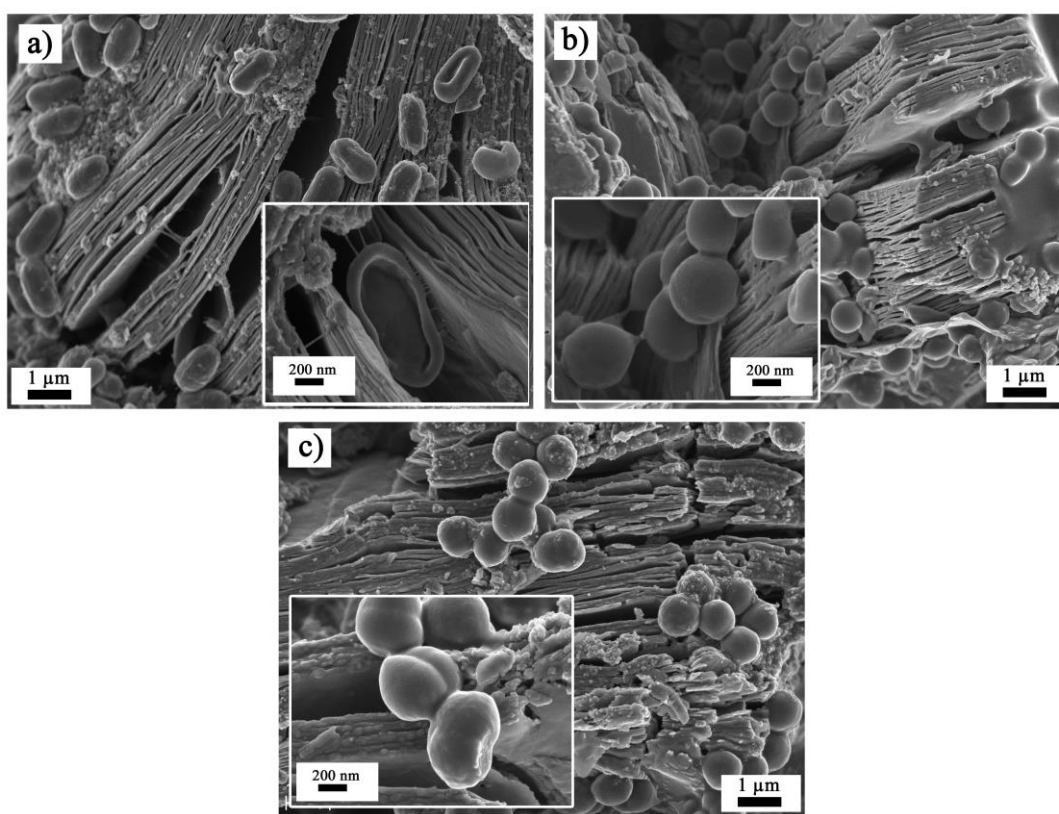


**Figure 9.** SEM images of the  $Ti_2C$  sheets with adsorbed bacteria cells such as: *Bacillus sp.* a), *S. aureus* b), and *Sarcina* c). The high magnification insets present in detail the adsorbed cells morphology.

The aim of this study was also to describe the preferential sites for adsorption of the bacteria cells on the surface of expanded  $Ti_2C$  using scanning electron microscope. The Fig. 9 shows the representative SEM images of the  $Ti_2C$  expanded sheets with the adsorbed bacteria cells of *Bacillus sp.*, *S. aureus*, and *Sarcina*. The morphology of the analysed cells was presented in detail on the high magnification insets. In case of *Bacillus sp.* species (Fig. 9a), the cells were randomly attached to the surface of the expanded walls of  $Ti_2C$ . However, one can notice that the cells also presented the specific ability to fit into the larger slit-shaped pores. The cells located between  $Ti_2C$  sheets were in

some cases highly disrupted. This effect was not seen for other bacteria species. The *S. aureus* and *Sarcina* cells were also found successfully attached to the surface of expanded  $Ti_2C$  sheets as can be seen in Fig. 8b and c, respectively. Their morphology was not significantly disrupted. However, in case of *S. aureus* some areas of the biofilm formed between individual  $Ti_2C$  sheets are present.

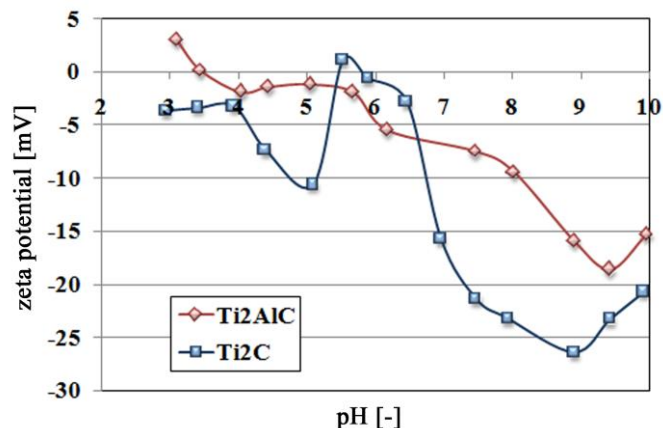


**Figure 10.** Zeta potential curves obtained for  $Ti_2AlC$  and expanded  $Ti_2C$  suspended in distilled water environment. The isoelectric points (IEPs) obtained for  $Ti_2AlC$  was 3,47 and for  $Ti_2C$  was 5,48 and 5,76.

In the next part of the study, the analysis of changes of zeta potential of  $Ti_2C$  as a result of bacteria cells adsorption was investigated. Such an analysis is very useful when there is a need for information on how the adsorption of bacteria cells changes the stability of a suspension and how much it influences the electrical charge formed on the surface of the analysed material or bacteria cells [7, 9, 10]. The methodology used for zeta potential investigations was similar to our previous reports [7, 11]. It should be also noted, that the  $Ti_2AlC$  was used as a reference only for the purpose of comparison of zeta potential of pure suspensions.

The zeta potential curves were recorded for the expanded  $Ti_2C$  and were presented in Fig. 10. It should be noted, that the  $Ti_2AlC$  sample was used in our investigations as a reference. It can be seen, that the zeta potential of  $Ti_2C$  was generally decreasing ca. -2,5 mV up to -26 mV when pH increased. However, it can be also noticed one clearly visible peak located around pH=6. Consequently, zeta potential curve two times crossed the zero zeta potential value. As a result, two IEPs (isoelectric points) were obtained i.e. 5,48 and 5,76. Moreover, at the highly basic environment (pH=ca. 9) the trend of the curve reversed and the zeta potential constantly increased with pH increase. When compare the shape of the zeta-curve to that obtained for  $Ti_2AlC$ , one can notice that it is closer to zero line without any peaks around pH=6. The IEP value obtained for  $Ti_2AlC$  was 3,47.

It should be however noted, that before our research there were no detailed reports on zeta potential curves of the expanded  $Ti_2C$ . To the best of our knowledge, there are only few reports available on other types of MXenes. Ren *et al.* [12] reported zeta potential of -29 mV at pH=7 for  $Ti_3C_2$  (IEP= 2.4). Ying *et al.* [13] found that the  $Ti_3C_2$  was characterized by a highly negative surface charge and the zeta potential of as-produced  $Ti_3C_2$  suspension was -39.5 mV. Authors assumed that the negative surface charge originated from the =O, -OH and -F terminating functional groups present

on the surface of  $Ti_3C_2$  sheets. Others researchers demonstrated that the  $V_2C$  sheets were negatively charged within the entire range of pH (from 0.97 to 11.3). At pH=7, the  $V_2C$  was found to possess highly negative surface charge (in the range from  $-46$  mV to  $-58$  mV) [14]. In contrast to those studies, the  $Ti_2C$  synthesized by us was characterized by a highly negative zeta potential only in the basic environment (in the 7-10 pH range). However, when the pH reached the value of 7, the rapid drop of zeta potential was observed.

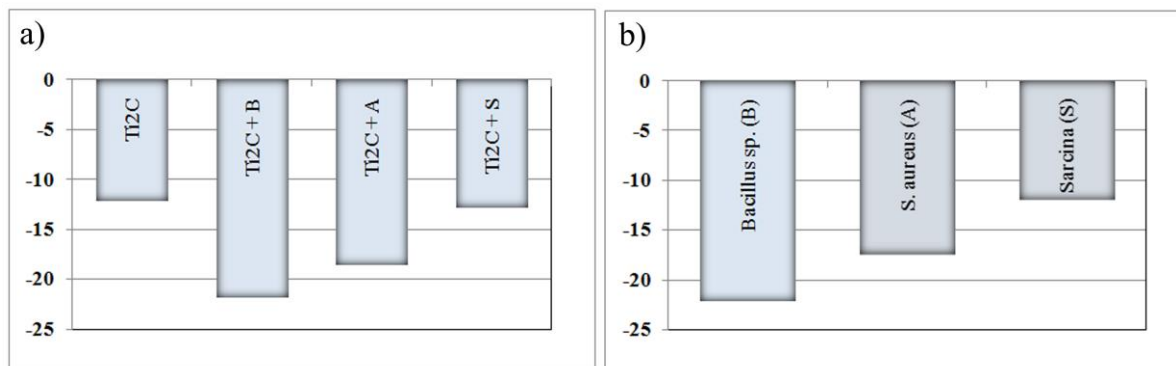


**Figure 11.** Zeta potentials obtained for the expanded  $Ti_2C$  with the presence of different bacteria cells a) as well as for pure bacteria cells suspensions in drinking water environment (pH=7,3) c). The bacteria strains were marked as: B for *Bacillus sp.*, A for *S. aureus* and S for *Sarcina*.

The zeta potentials obtained for  $Ti_2C$  suspensions in drinking water without and with the presence of bacteria cells were presented in Figure 11. The  $Ti_2C$  suspension was used in this study as a reference (Fig. 11 a). The pure suspensions of particular bacteria cells of strains such as: *Bacillus sp.*, *S. aureus* and *Sarcina* were presented in Fig. 11 b. We expected that the adsorption of bacteria cells onto the surface of  $Ti_2C$  should change its surface charge to similar to adsorbed cells by simple adjustment of the potential as a result of covering of the adsorbent surface [7, 9]. Our results indicate, that the adsorption of bacteria cells on the surface of  $Ti_2C$  resulted in adjustment of its zeta potential to that of bacteria cells. Thus, our results are in agreement with other data [7, 9]. It is known that during bacterial adhesion the electric double layer interactions lead to the redistribution of charges and the heterogeneous distribution of charges on the surface of bacteria reduces the effect of double layer repulsion during bacterial adhesion without affecting of bacteria viability [15]. Also the ion-penetrable layer of surface polymeric groups that are known to exist on the surface of bacteria may increase the attractive steric interactions promoting the adhesion by bridging the gap between two surfaces that repel each other (the ‘bridging’ interactions) [15]. All the mentioned phenomena could interplay on the surface of tested bacteria due to achieve the adsorption on the surface of  $Ti_2C$ .

#### 4. SUMMARY

Recently, the chemically expanded structures of early transition metal carbides, known as MXenes have been introduced together with their specific properties which can be described as characteristic for both metals and ceramics. It made them attractive in the high-tech area of science. However, the potential of the biological activity of MXenes have not yet been fully discovered, highly

limiting the possibility of their application in many fields of bioscience and biotechnology. The present study, for the first time, investigates the biological activity of  $Ti_2C$ , which is the expanded form of layered titanium carbide ( $Ti_2AlC$ ) against the gram-positive bacteria commonly occurring in the natural environment such as: *Bacillus sp.*, *S. aureus* and *Sarcina*. The aim of this study was also to describe the preferential sites for adsorption of the bacteria cells using scanning electron microscope examinations as well as analysis of changes of zeta potential of expanded  $Ti_2C$  MXene as a result of bacteria cells adsorption.

The SEM investigations results have shown that the layers of the dense  $Ti_2AlC$  grains were successfully split into individual sheets of the expanded  $Ti_2C$  characterized by the extended widths of the grains located perpendicular to the surface of the sheets. The diameters of the individual sheets varied between 26 and 61 nm. The sheets were also connected to each other forming the specific stack of nano-sized sheets with the pores of slit-type. The EDS results revealed that the amount of aluminium was reduced from c.a. 17 wt% in  $Ti_2AlC$  to almost 0 wt% in  $Ti_2C$  which confirmed the efficiency of the chemical process of aluminium extraction from  $Ti_2AlC$ . The presence of significant amounts of oxygen and fluorine was also confirmed. The shape of the isotherms obtained for the expanded  $Ti_2C$  suggested the presence of slit-shaped pores in the size range of 3–5 nm. As expected, the BET specific surface area of expanded  $Ti_2C$  was ca. 42% higher in comparison with layered  $Ti_2AlC$ .

It was also revealed, that both  $Ti_2AlC$  and  $Ti_2C$  did not influence negatively the analyzed gram-positive bacteria. Moreover, the slightly intensified growth of gram-positive *Bacillus sp.* strain was observed in the vicinity of tested  $Ti_2AlC$  and  $Ti_2C$ . What is interesting, this effect was not revealed for other gram-positive *S. aureus* and *Sarcina* strains. It should be noted, that the SEM investigations of the preferential sites for bacteria adsorption indicated the presence of minor apoptosis only for *Bacillus sp.* strain, especially when the cells were located between individual sheets of the expanded  $Ti_2C$ . The analysis of changes of zeta potential of  $Ti_2C$  in the presence of bacteria has shown that adsorption of bacteria cells on the surface of  $Ti_2C$  resulted in changing of its zeta potential to that of bacteria cells.

#### ACKNOWLEDGEMENTS

The scientific work was financed from the budget for science in the years 2016-2019, decision no. 0277/IP2/2016/74, 24.08.2016 (Ministry of Science and Higher Education).

*The authors declare that there is no conflict of interest regarding the publication of this paper.*

#### References

1. M. W. Barsoum, *Prog. Solid State Chem.* 28 (2000) 201.
2. M. Naguib, O. Mashtalir, J. Carle, V. Presser, J. Lu, L. Hultman, *ACS Nano* 6 (2012) 1322.
3. M. Naguib, V. N. Mochalin, M. W. Barsoum, Y. Gogotsi, *Adv. Mat.* 26 (2014) 992.
4. O. Mashtalir, M. Naguib, B. Dyatkin, Y. Gogotsi, M. W. Barsoum, *Mat. Chem. Phys.* 139 (2013) 147-152.
5. F. Wang, C. H. Yang, C. Y. Duan, D. Xiao, Y. Tang, J. F. Zhu, *J. Electrochem. Soc.* 162 (2015) B16.
6. X. Xie, S. Chen, W. Ding, Y. Nie, Z. Wei, *Chem. Commun.* 49 (2013) 10112.

7. A. M. Jastrzębska, E. Karwowska, P. Kurtycz, A. R. Olszyna, A. Kunicki, *Surf. Coat. Technol.* 271 (2015) 225.
8. A. M. Jastrzębska, J. Jureczko, A. R. Kunicki, A. R. Olszyna, *Int. J. Appl. Ceram. Technol.* 12 (2015) 522.
9. A. Jastrzębska, E. Karwowska, A. Olszyna, Chapter XI - Bio-Assessment and Toxicology: Influence of the Staphylococcus Aureus Bacteria Cells on the Zeta Potential of Graphene Oxide Modified with Alumina Nanoparticles in Electrolyte and Drinking Water Environment. In *Springer Proceedings in Energy, 2nd International Congress on Energy Efficiency and Energy Related Materials (ENEFM 2014)*, Oludeniz, Fethiye/Mugla, Turkey, 2014, pp 245-250.
10. P. Kurtycz, A. M. Jastrzębska, E. Karwowska, A. Olszyna, A.; Comparative assessment of the Graphene oxide and reduced Graphene oxide influence on the zeta potential of selected bacteria in drinking water environment. *Proceedings of the 9th International Conference on Composite Science and Technology (ICCST) – 2020 – Scientific and Industrial Challenges*, Naples, Italy, 2013, pp 383-393.
11. A. M. Jastrzębska, E. Karwowska, P. Kurtycz, E. Miałkiewicz-Pęska, D. Basiak, A. Olszyna, M. Załęska-Radziwiłł, N. Doskocz, *Int. J. Appl. Ceram. Technol.* 12 (2015) 1157.
12. C. E. Ren, K. B. Hatzell, M. Alhabeab, Z. Ling, K. A. Mahmoud, Y. Gogotsi, *J. Phys. Chem. Lett.* 6 (2015) 4026.
13. Y. Ying, Y. Liu, X. Wang, Y. Mao, W. Cao, P. Hu, X. Peng, *ACS Appl. Mat. Interfaces* 7 (2015) 1795.
14. M. Naguib, R. R. Unocic, B. L. Armstrong, J. Nanda, *Dalton Trans.* 44 (2015) 9353.
15. A. T. Poortiga, R. Bos, W. Norde, H. J. Busscher, *Surf. Sci. Rep.* 47 (2002) 1.

© 2017 The Authors. Published by ESG ([www.electrochemsci.org](http://www.electrochemsci.org)). This article is an open access article distributed under the terms and conditions of the Creative Commons Attribution license (<http://creativecommons.org/licenses/by/4.0/>).